Wang, A. H.-J., Fujii, S., van Boom, J. H., & Rich, A. (1982) *Proc. Natl. Acad. Sci. U.S.A. 79*, 3968–3972.
Wang, A. H.-J., Gao, Y.-G., Liaw, Y.-C., & Li, Y.-K. (1991) *Biochemistry 30*, 3812–3815.
Westhof, E., Dumas, P., & Moras, D. (1985) *J. Mol. Biol. 184*, 119–145.
Yanagi, K., Prive, G., & Dickerson, R. E. (1991) *J. Mol. Biol. 217*, 201–214.

Characterization of Conformational Features of DNA Heteroduplexes Containing Aldehydic Abasic Sites†

Jane M. Withka, Joyce A. Wilde, and Philip H. Bolton*
Department of Chemistry, Wesleyan University, Middletown, Connecticut 06459
Abhijit Mazumder and John A. Gerlt
Department of Chemistry and Biochemistry, University of Maryland, College Park, Maryland 20742
Received May 16, 1991; Revised Manuscript Received July 17, 1991

ABSTRACT: The DNA duplexes shown below, with D indicating deoxyribose aldehyde abasic sites and numbering from 5′ to 3′, have been investigated by NMR. The ^{31}P and ^{31}P–^{1}H correlation data indicate

$d(C_1\ G_2\ C_3\ A_4\ G_5\ D_6\ C_7\ A_8\ G_9\ C_{10}C_{11})$
$d(G_{22}C_{21}G_{20}T_{19}C_{18}A_{17}G_{16}T_{15}C_{14}G_{13}G_{12})$

$d(C_1\ G_2\ C_3\ A_4\ G_5\ D_6\ C_7\ A_8\ G_9\ C_{10}C_{11})$
$d(G_{22}C_{21}G_{20}T_{19}C_{18}G_{17}G_{16}T_{15}C_{14}G_{13}G_{12})$

that the backbones of these duplex DNAs are regular. One- and two-dimensional ^{1}H NMR data indicate that the duplexes are right-handed and B-form. Conformational changes due to the presence of the abasic site extend to the two base pairs adjacent to the lesion site with the local conformation of the DNA being dependent on whether the abasic site is in the α or β configuration. The aromatic base of residue A17 in the position opposite the abasic site is predominantly stacked in the helix as is G17 in the analogous sample. Imino lifetimes of the AT base pairs are much longer in samples with an abasic site than in those containing a Watson–Crick base pair. The conformational and dynamical properties of the duplex DNAs containing the naturally occurring aldehyde abasic site are different from those of duplex DNAs containing a variety of analogues of the abasic site.

The in vivo repair of chemical damage to the bases in DNA as well as the misincorporation of bases that can occur during replication is frequently initiated by the hydrolysis of the N-glycosyl bond to yield an abasic site (Lindahl, 1982; Friedberg, 1985; Loeb & Preston, 1987). For example, the spontaneous deamination of cytosine to uracil occurs at a genetically significant rate, and the resulting uracil is removed by uracil-DNA glycosylase to produce an abasic site. The abasic site is an equilibrium mixture of α- (I) and β- (II) hemiacetals (2-deoxy-D-*erythro*-pentofuranoses), aldehyde (III), and hydrated aldehyde (IV), as depicted in Scheme I. The hemiacetal forms predominate, with about 1% aldehyde being present (Manoharan et al., 1988a; Wilde et al., 1989). The strand cleavage at the 3′-side of the abasic site catalyzed by UV endonuclease V of bacteriophage T4 or endonuclease III of *Escherichia coli* occurs via a syn β-elimination reaction (Manoharan et al., 1988b; Mazumder et al., 1989, 1991). The hydroxide-catalyzed reaction proceeds via an anti β-elimination reaction (Mazumder et al., 1991).

Scheme I

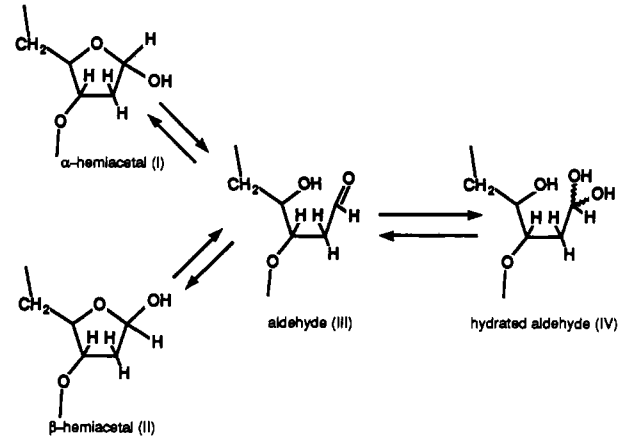

We have previously examined duplex heptamers containing aldehyde abasic sites (Manoharan et al., 1988a,b; Mazumder et al., 1989; Wilde et al., 1989), but these do not have sufficient thermal stability for detailed characterization by NMR. Thus, samples of the DNA heteroduplex

$d(C_1\ G_2\ C_3\ A_4\ G_5\ D_6\ C_7\ A_8\ G_9\ C_{10}C_{11})$
$d(G_{22}C_{21}G_{20}T_{19}C_{18}A_{17}G_{16}T_{15}C_{14}G_{13}G_{12})$

numbering from 5′ to 3′, have been prepared by methods

† This research was supported, in part, by Grant NP-750 from the American Cancer Society (P.H.B.) and by the Bristol-Myers Squibb Corp. via participation in a State of Connecticut Cooperative High Technology Research and Development Grant (P.H.B.). J.M.W. is a recipient of a traineeship in molecular biophysics via NIH 1T32 GM-08271 (P.H.B.).

0006-2960/91/0430-9931$02.50/0

described previously (Manoharan et al., 1988a,b; Mazumder et al., 1989; Wilde et al., 1989); this heteroduplex is referred to as AD1. The properties of the related DNA heteroduplex sample containing G opposite the abasic site

$$d(C_1\ G_2\ C_3\ A_4\ G_5\ D_6\ C_7\ A_8\ G_9\ C_{10}C_{11})$$
$$d(G_{22}C_{21}G_{20}T_{19}C_{18}G_{17}G_{16}T_{15}C_{14}G_{13}G_{12})$$

referred to here as GD1, have also been investigated as well as those of the "control sample" of the analogous duplex not containing an abasic site

$$d(C_1\ G_2\ C_3\ A_4\ G_5\ U_6\ C_7\ A_8\ G_9\ C_{10}C_{11})$$
$$d(G_{22}C_{21}G_{20}T_{19}C_{18}A_{17}G_{16}T_{15}C_{14}G_{13}G_{12})$$

which is referred to as AU1. As demonstrated below, both GD1 and AD1 have sufficient thermal and chemical stability for NMR analysis.

These sequences were chosen to have a high GC content to maximize stability and to have no runs of dA or other features that are known to have a preference for special conformational features. The sequences were also designed to have low symmetry to preclude self association. In addition, the top strand of the sequences can be extended to give GGTACCGC... U...GCCCCCGGG, which has a *Kpn*I site on the 5′ side and an *Ava*I site on the 3′ side. This will allow the sequences studied here by physical methods to also be used in experiments on the abasic sites in vivo.

The base opposite the abasic site is of interest since there are several possible naturally occurring and induced routes by which an abasic site can be generated. Having dG opposite the abasic site can be obtained following deamination of a dC residue followed by the action of N-uracil-DNA glycosylase, which occurs at a genetically significant rate (Lindahl, 1982; Friedberg, 1985; Loeb & Preston, 1987), and hence GD may be the most common naturally occurring case. The base opposite the abasic site may have structural, dynamical, or other properties which affect the chemical reactivity of the duplex DNA, its recognition by proteins, or its interactions in subsequent repair reactions.

The base opposite the abasic site is of interest in understanding the role of abasic sites in mutagenesis. When DNA polymerase copies DNA containing an abasic site there is a strong preference, about 90%, for dA to be put in the daughter strand in the position opposite the abasic site (Lindahl, 1982; Friedberg, 1985; Loeb & Preston, 1987; Schaaper et al., 1983; Sagher & Strauss, 1983; Randall et al., 1987). If it could be determined that there are special structural, hydrogen-bonding, or dynamical features associated with dA interacting with the abasic site, then these physical properties potentially could be related to the dA preference, which occurs during the rate-determining step in the polymerase reaction. On the other hand, if the various bases have similar interactions with the abasic site in the context of duplex DNA, then the preference for dA is most likely that of the replication complex.

There have been a number of studies of DNA duplexes containing analogues of the naturally occurring aldehydic abasic site (Cuniasse et al., 1987, 1990; Kalnik et al., 1988, 1989). These studies have been concerned with the tetrahydrofuran analogue or other analogues that differ from the aldehydic abasic site in hydrogen-bonding potential, chemical reactivity, and perhaps other properties as well. The hydrogen-bonding potential may be important since it is likely that the abasic site interacts with water molecules. Unless the DNA helix is severely distorted, there can be no direct interaction between the sugar at the abasic site and the base on the opposing strand. While it has been shown that DNA duplexes containing the tetrahydrofuran analogue can be substrates for certain enzymes (Kalnik et al., 1988, 1989), it is not known whether the structural and dynamical properties of duplexes containing aldehydic abasic sites are similar to those of DNA duplexes containing an analogue of the abasic site. A recent investigation by Serianni and co-workers indicates that the conformational preferences of at least some abasic site analogues are different from those of the naturally occurring material (Serianni et al., 1990).

Studies on aldehydic abasic sites are also of interest as they relate to studies on DNA degradation by drugs such as bleomycin and neocarzinostatin, which are known to abstract protons from the deoxyribose of DNA (Goldberg, 1987; Kozarich et al., 1989; Kappen et al., 1991). These reactions lead to products such as deoxyribolactones and other types of non-aldehydic abasic sites that contain an altered sugar and no base. The results obtained for aldehydic abasic sites may be useful for comparison with those generated by antitumor and other drugs.

This investigation compares the results from NMR experiments on the abasic-site-containing heteroduplexes AD1 and GD1 with those of AU1 to ascertain the range and magnitudes of the structural and dynamical effects of the presence of an abasic site as well as the differences that may be due to the nature of the base opposite the abasic site. Furthermore, the properties of these DNAs containing aldehydic abasic sites will be compared with results previously obtained on DNA duplexes containing analogues of the aldehydic abasic site to ascertain the relevance of the results obtained on the model systems.

Experimental Procedures

Sample Preparation. DNA single strands were synthesized by the solid-phase phosphoramidite method on an Applied Biosystems 381A automated DNA synthesizer on the 10-μmol scale. Single-stranded DNA was deprotected and purified by dialysis and reverse-phase HPLC on a preparative Hamilton PRP-1 column and eluted with a gradient of 1.5–8.5% acetonitrile in 25 mM phosphate buffer, pH 7.0, in 22.5 min. The DNA was then dialyzed and its extinction coefficient determined via the total phosphorus method. The single strands were lyophilized and reconstituted in pH 7.0 buffer containing 10 mM sodium phosphate, 100 mM sodium chloride, and 0.05 mM EDTA in 99.96% ^2H_2O.

The abasic site single strands were prepared by treating DNA single strands containing a single U residue with N-uracil glycosylase as described previously (Manoharan et al., 1988a,b; Mazumder et al., 1989; Wilde et al., 1989). The extent of reaction was monitored during the reaction by the reverse-phase HPLC method described above, which separates free uracil, the DNA single strand containing U, and the DNA single strand containing the abasic site. The single strand containing the abasic site was purified by gel-filtration chromatography on a preparative TSK-GEL G2000SW column and eluted with 25 mM sodium phosphate buffer and 100 mM sodium chloride at pH 7.0 to remove N-uracil glycosylase and free uracil. The purified single strand was subsequently dialyzed, lyophilized to dryness, and redissolved in pH 7.0 buffer containing 10 mM sodium phosphate, 100 mM sodium chloride, and 0.05 mM EDTA in 99.96% ^2H_2O. Abasic site containing single-stranded DNA prepared by this approach was found to be pure by both proton and ^{31}P NMR and to be free of phosphodiester cleavage products. Overall yield for the conversion of the single-stranded material to abasic site containing DNA was about 85%. Due to the degradation of single-stranded DNA containing abasic sites at elevated tem-

peratures with subsequent irreversibility of duplex formation, precise melting temperatures for AD1 and GD1 were not determined.

The heteroduplexes were formed by mixing equimolar quantities, based on the extinction coefficients of the two strands, and by monitoring the titration of the single strand containing the residue dU or D with the adjacent strand. The duplex was lyophilized several times in ^2H_2O and redissolved in 0.4 mL of 99.96% ^2H_2O. The purified duplex was studied at 1–1.5 mM concentration in pH 7.0 buffer containing 10 mM sodium phosphate, 100 mM sodium chloride, and 0.05 mM EDTA in 99.96% ^2H_2O. For one-dimensional NMR experiments involving the exchangeable imino protons, the duplex was lyophilized and redissolved in 90% H_2O/10% ^2H_2O.

NMR Procedures. The 600-MHz NMR spectra were obtained by using a Varian Unity spectrometer with the assistance of Drs. George Gray and Paul Kiefer of Varian Associates. The 400-MHz NMR spectra were obtained by using a Varian XL-400 spectrometer, as were the ^{31}P and ^{31}P–^1H correlation spectra. All data were analyzed by Varian VNMR software on a Sun Microsystem 3/280S. The two-dimensional NOE spectra were obtained as described elsewhere (Ernst et al., 1987), as were the DQF-COSY (Braunschweiler & Ernst, 1983; Wüthrich, 1986; Chazin et al., 1986), TOCSY (Braunschweiler & Ernst, 1983; Shaka et al., 1988), and ROESY (Bothner-By et al., 1983; Bax & Davis, 1985) two-dimensional data, the one-dimensional temperature dependence runs, and the imino proton T_1 data (Leroy et al., 1988; Pardi et al., 1982). All two-dimensional data were obtained by using the States–Haberkorn hypercomplex method (States & Haberkorn, 1982).

Heteronuclear ^{31}P–^1H correlation data were obtained by using the pulse sequence

$$\begin{array}{lcccc} ^1H: & 90°\text{–}\tau\text{–} & -t_1/2\text{–}180°\text{–}t_1/2\text{–} & \text{–acquisition} \\ ^{31}P: & \text{–}90°\text{–} & \text{–}90°\text{–} & \end{array}$$

This pulse sequence gives rise to a phase-sensitive two-dimensional map in which the F_1 axis is the phosphorus chemical shift and the F_2 axis is the proton chemical shift. The τ delay time was 20 ms. This procedure was found to be more sensitive than previously proposed methods and will be described in detail elsewhere.

The 2D NOE spectra were acquired at 600 MHz, 20 °C, and mixing times of 120 and 360 ms. The water resonance was presaturated during the 1-s delay between acquisitions. Sixty-four acquisitions for each of the 256 t_1 values were collected with 4K points for the duplex AD1. For AU1, 64 acquisitions for each of the 512 t_1 values were collected with 2K points, and for GD1, 128 acquisitions for each of 280 t_1 values were collected with 4K points. In all experiments, the free induction decay, fid, along t_1 was zero-filled to 2K data points prior to Fourier transformation to give a final 2K × 2K spectrum. Data processing was optimized for each experiment and included Gaussian apodization and Gaussian shift constant in t_1 and t_2 for resolution enhancement and drift correction, with a first-order polynomial, in both the F_1 and F_2 dimensions. The GD1 two-dimensional data were processed with the use of a sine bell function as well.

The DQF-COSY spectra were collected at 400 MHz and 20 °C for AD1, AU1, and GD1. In these experiments, 128 acquisitions for each of the 512 t_1 values were obtained with 2K points. The fid along t_1 was zero-filled to 2K data points prior to Fourier transformation to give a final 2K × 2K spectrum. The data were processed with Gaussian apodization and Guassian shift constant in t_1 and t_2 and drift corrected in both dimensions.

ROESY experiments were performed at 400 MHz and 20 °C for AD1 at mixing times of 90 and 120 ms and a delay time of 1 s between scans. In these experiments, 128 acquisitions for each of the 256 t_1 values were obtained with 2K points. The fid along t_1 was zero-filled to 2K data points prior to Fourier transformation to give a final 2K × 2K spectrum. The data were processed with Gaussian apodization and Gaussian shift constant in t_1 and t_2 and drift corrected.

The TOCSY spectra were obtained at 400 MHz and 20 °C for AD1 with mixing times of 50 and 60 ms and a delay time of 1 s between acquisitions. The DIPSI-2 decoupling scheme was employed to generate the spin lock during the mixing time (Shaka et al., 1988). The use of a long pulse in the DIPSI-2 improved the spin locking through the minimization of inhomogeneity effects (Shaka et al., 1983). In these experiments, 96 acquisitions for each of the 512 t_1 values were collected with 2K data points. The fid along t_1 was zero-filled to 2K data points to give a final 2K × 2K spectrum. The data were processed with Gaussian apodization and Gaussian shift constant in t_1 and t_2 and drift corrected in both dimensions.

The heteronuclear ^{31}P–^1H experiment described above was obtained at 400 MHz and 20 °C for AD1. In this experiment, 1024 acquisitions for each of the 32 t_1 values were collected with 2K data points. The data were processed with Gaussian apodization and Gaussian shift constant in t_1 and t_2. The data were baseline corrected with a ninth-order polynomial along F_2 and drift corrected along F_1.

The one-dimensional ^1H spectra for the nonexchangeable protons of AD1, AU1, and GD1 were carried out at 400 MHz and at temperatures between 10 and 25 °C. One-dimensional ^1H spectra for the exchangeable imino protons of AD1, AU1, and GD1 were obtained at 400 MHz and at temperatures between −0.5 and 25 °C. A 1–1 observe pulse was used for water suppression (Hore, 1983). Imino proton longitudinal relaxation time, T_1, experiments were performed at 400 MHz and at temperatures between 10 and 20 °C. T_1s were determined by selective saturation recovery methods with a range of appropriate delay times. A 1–1 observe pulse was used for water suppression.

Results

NMR Studies of AD1 and GD1. The assignment procedure for DNA duplexes containing aldehydic abasic sites presented several potential difficulties. The abasic sites were expected to be present in both the α and β configurations and hence two closely related DNA molecules would be present in solution. This could lead to relatively complicated spectra such that the making of assignments could be quite challenging. Similarly, it was plausible the base opposite the abasic site might be in an equilibrium between extrahelical and stacked forms, which could also lead to multiple sets of signals. The other potential difficulty was that there would not be sufficient NOE connectivities through the abasic site to allow for sequential assignments.

As described below, the AD1 proton spectrum could be assigned via sequential assignments by obtaining two-dimensional spectra at the highest available field strength as well as exploiting the information from a variety of two-dimensional experiments performed at lower field strength. The results indicate that AD1 is basically a B-form DNA with some distortion in the region of the lesion, apparently limited to the base pairs adjacent to the abasic site. The α configuration of the abasic site exists as a single conformer, whereas two forms of the β configuration exist in solution and chemical

Table I: AD1 Chemical Shift Assignments[a]

residue	H_6/H_8	H_5	$H_{1'}$	$H_{2'}$	$H_{2''}$	$H_{3'}$	$H_{4'}$	CH_3
C1	7.77	6.05	5.89	2.11	2.54	4.83	nya	
G2	8.09		6.01	2.80	2.84	5.10	4.47	
C3	7.51	5.59	5.63	2.09	2.42	4.48	4.28	
A4[b]	8.26		6.13	2.79	2.95	5.15	4.49	
G5[c]	7.84, 7.85		5.99, 6.03	2.61	2.66	5.09	4.45	
D6(α)			5.58	2.12	2.32	4.70	nya[d]	
D6(β)			5.63	2.04	2.33	4.65 (1), 4.53 (2)	nya	
C7[c]	7.78, 7.75	6.08, 6.01	5.69, 5.70	2.14	2.49, 2.48	4.50	4.32	
A8	8.36		6.06	2.89	2.99	5.15	4.49	
G9	7.82		5.89	2.66	2.75	5.06	4.49	
C10	7.52	5.27	6.10	2.24	2.57	4.87	4.27	
C11	7.78	5.88	6.35	2.47	2.38	4.66	4.14	
G12	8.01		5.84	2.70	2.85	4.99	4.32	
G13	8.01		6.12	2.82	2.88	5.13	4.55	
C14	7.57	5.28	6.14	2.15	2.60	5.13	4.37	
T15[b]	7.40		5.78	2.06	2.36	nya	4.21	1.76
G16[c]	7.90, 7.91		5.65, 5.72	2.69, 2.73	nya, nya	5.07, 5.08	4.35, 4.38	
A17[c]	8.21		6.20, 6.22	nya	2.79	5.03, 5.03	4.50	
C18[c]	7.61, 7.66	5.62, 5.68	5.91, 5.91	2.18, 2.21	2.51, 2.52	4,87, 4.87	4.30, 4.31	
T19	7.49		5.83	2.24	2.56	4.97	4.26	1.76
G20	8.05		6.01	2.80	2.84	5.11	4.50	
C21	7.48	5.59	5.89	2.03	2.46	5.10	nya	
G22	8.07		6.28	2.74	2.49	4.80	4.30	

[a] H_2O is referenced at 4.90 ppm. [b] Proton with two signals unresolved in two-dimensional data. [c] Proton with two resolved signals in two-dimensional data. [d] nya, proton signal not yet assigned.

exchange between them can be observed.

The imino proton results show that the presence of an abasic site reduces the rate of imino proton exchange with solvent. This surprising result was observed both with AD1 and GD1 relative to the AU1 sample.

The ^{31}P studies confirmed that the DNA duplexes containing aldehydic abasic sites are generally B-form and that there is not significant distortion in the area adjacent to the abasic site. This is in contrast to results previously obtained on DNA duplexes containing analogues of the abasic site (Kalnik et al., 1988, 1989).

Proton Assignments of AD1. The proton NMR spectrum of AD1 was assigned by means of sequential assignments (Wemmer & Reid, 1985; Wüthrich, 1986; Clore & Gronenborn, 1989; Bolton, 1990). The resolution of 600-MHz NOE data allowed the assignments of most aromatic, $H_{1'}$, $H_{2'}$, $H_{2''}$, $H_{3'}$, and $H_{4'}$ protons by the methods described below. The assignments of AD1 were further confirmed by 400-MHz DQF-COSY, ROESY, and TOCSY data and are presented in Table I. The two-dimensional NOE data for AD1 showed the familiar connectivities associated with B-form DNA. The region of the two-dimensional map shown in Figure 1a contains the intraresidue aromatic to $H_{2'}$ and $H_{2''}$ cross-peaks and the interresidue 3′ aromatic to 5′ $H_{2''}$ cross-peaks for AD1. As an example, the interresidue 3′ aromatic to 5′ $H_{2''}$ connectivities for C18 ⇒ A17 ⇒ G16 ⇒ T15 ⇒ C14 ⇒ G13 are shown. Many of the interresidue 3′ aromatic to 5′ $H_{2'}$ cross-peaks are also observed due to significant spin diffusion at the mixing times used. These connectivities were verified by the intraresidue aromatic to $H_{1'}$ cross-peaks and the interresidue 3′ aromatic to 5′ $H_{1'}$ cross-peaks shown in Figure 1b. Interresidue aromatic to sugar connectivities were observed for all residues in AD1 with the exception of D6 ⇒ G5, in which the base of D6 has been removed to form the abasic lesion, and G13 ⇒ G12, in which the H_8 protons are degenerate. Although the intensities of the NOEs have not been quantified due to the significant spin diffusion at the experimental mixing times, the intensities of the aromatic to ribose cross-peaks appear qualitatively similar for all residues. All glycosyl torsion angles are in the anti conformation as evidenced by the moderate intensity for the intraresidue aromatic to $H_{1'}$ NOE relative to the strong intensity of the H_6 to H_5 NOE (Kalnik et al., 1989). The moderate intensity observed corresponds to an estimated interproton distance of greater than 3.0 Å, which is characteristic of the anti configuration. These data indicate that AD1 is a fairly regular B-form duplex.

Findings by interpretation of two-dimensional NMR data include the observation of two sets of signals for several of the protons of the residues G5, D6, C7, C18, A17, and G16, which correspond to the presence of both anomeric forms of the abasic site. These residues belong to the base pair involving the abasic site and those directly adjacent to the site. As an example, two H_6 protons for C18 can be observed in Figure 1a. Both forms show connectivity to intraresidue $H_{2'}/H_{2''}$ protons and to the $H_{2''}$ proton of A17. In addition, the H_6 of C18 shows connectivity to the methyl protons of T19. In Figure 1b, multiple forms of the H_6 and H_5 protons of C7 and C18 and the H_8 and $H_{1'}$ protons of G16 are shown. Multiple sets of signals were confirmed for C7 and C18 in the H_6 to H_5 region in the 400-MHz DQF-COSY spectra (see supplementary material). The interresidue connectivities involving multiple forms are similar, indicating that both forms of the duplex are structurally similar. The only exception is the C7 aromatic to D6 sugar connectivities in which the $H_{1'}$ proton is in a different physical and chemical environment in the α and β anomeric forms.

The $H_{1'}$ to $H_{2'}/H_{2''}$ connectivities in the NOESY and DQF-COSY spectra verified the sugar proton assignments obtained as described above for each residue. The $H_{3'}$ protons were assigned on the basis of aromatic to $H_{3'}$ cross-peaks and verified by the observable $H_{1'}$ to $H_{3'}$ and $H_{2'}/H_{2''}$ to $H_{3'}$ cross-peaks. The $H_{4'}$ protons of these residues were also assigned by the aromatic to $H_{4'}$ cross-peaks in the NOESY spectra and were confirmed by the $H_{1'}$ to $H_{4'}$ cross-peaks in the ROESY spectra.

The $H_{1'}$ to $H_{2'}/H_{2''}$ region is shown in Figure 2a with the signals from the $H_{1'}$–$H_{2'}$ and $H_{1'}$–$H_{2''}$ cross-peaks of the two anomeric forms of the abasic site designated. The upfield signal at 5.58 ppm is due to the $H_{1'}$ proton of the α form, and the downfield signal at 5.63 ppm is due to the $H_{1'}$ proton of the β form of the abasic site. The same numbering system is used for the abasic site as for the other deoxyriboses. These

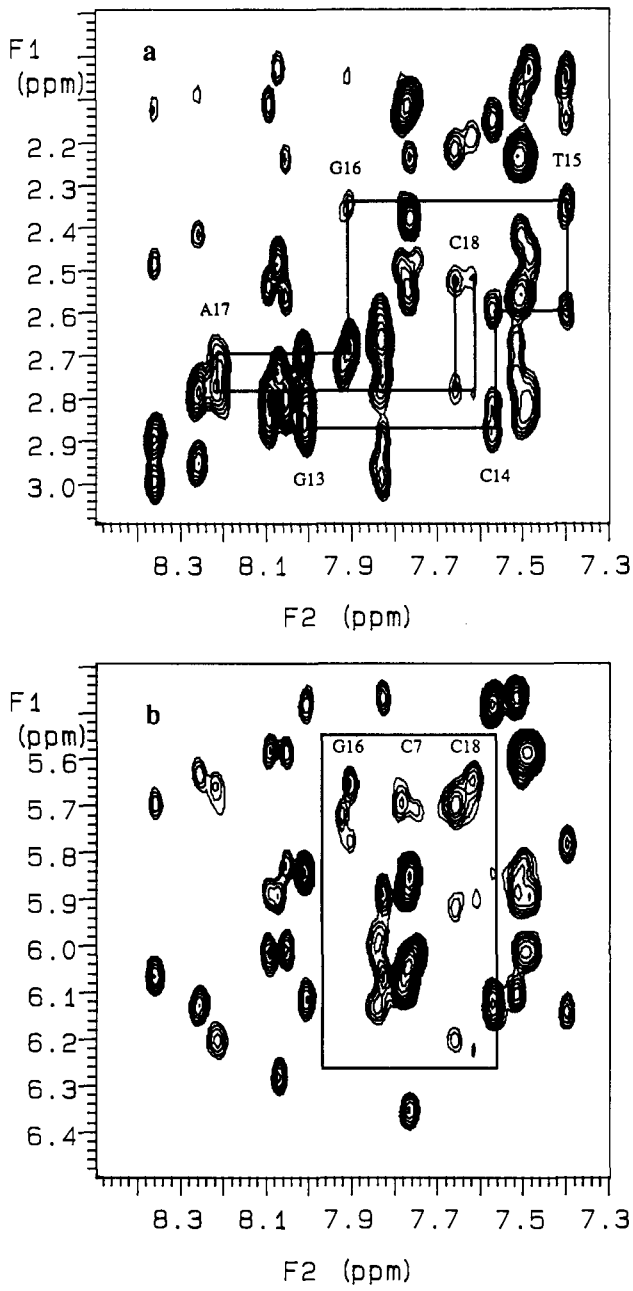

FIGURE 1: Two-dimensional 600-MHz NOESY spectra of AD1 at 20 °C and a mixing time of 360 ms. In (a) the $H_{2'}/H_{2''}$ to aromatic region with interresidue 3′ aromatic, H_6 or H_8, to 5′ $H_{2''}$ connectivities for the residues C18-A17-G16-T15-C14-G13 are shown. Multiple signals for the H_6 proton of C18 are observed. In (b) the $H_5/H_{1'}$ to aromatic region with multiple signals for the H_6 and H_5 protons of C18 and C7 and the H_8 and $H_{1'}$ protons of G16 are indicated. All of the spectra are referenced with H_2O at 4.90 ppm.

cross-peaks occur in a relatively well resolved region of the two-dimensional NOE map as shown in Figure 2a, with the exception of the $H_{1'}$ to $H_{2'}$ cross-peak of the α anomeric form, which lies in the identical region as H_5 to $H_{2'}/H_{2''}$ cross-peaks of C3 and C21. In the TOCSY spectrum shown in Figure 2b, only coupled spin systems are observed and the cross-peaks due to the H_5 of C3 and C21 were eliminated, thus allowing for proper assignments of the $H_{2'}$ of the α anomeric form. The ROESY spectrum, shown in Figure 2c, contains only direct diffusion cross-peaks, and as a consequence, only the $H_{1'}$ to $H_{2''}$ cross-peaks are observed at the experimental mixing times.

The $H_{3'}$ protons for the abasic site were assigned on the basis of the data described below. Three signals for the $H_{3'}$ protons of the abasic site could be identified. The most downfield of these signals could be correlated to the $H_{2'}$ and $H_{2''}$ protons of the α anomeric form. This $H_{3'}$ proton could also be correlated to the most upfield H_5 of C7. For the β anomeric form, two $H_{3'}$ resonances, associated with a major and a minor form, were observed to be correlated with the $H_{2'}$ and $H_{2''}$ protons of the β form. These two $H_{3'}$ protons were found to be in chemical exchange by ROESY and NOESY experiments as shown in Figure 3. The major form of the $H_{3'}$ proton was found to be correlated to the most downfield H_5 of C7. It is unknown if the minor form is also correlated to the H_5 of C7 since the potential cross-peak is in an unresolved region. It is noted that the differences in chemical shifts of the $H_{1'}$, $H_{2'}$, $H_{2''}$, and $H_{3'}$ protons between the two configurations is essentially the same in the heteroduplex environment as previously found for the free deoxyribose (Serianni et al., 1990). The $H_{4'}$ protons for the α and β anomeric forms of the abasic site have not been assigned as yet. Chemical exchange was not observed by two-dimensional NOESY and ROESY methods for the $H_{1'}$, $H_{2'}$, $H_{2''}$, and $H_{3'}$ protons of the α and β anomeric forms of D6. These results indicate the exchange rate for the $\alpha \Leftrightarrow \beta$ conversion is relatively slow at 20 °C, as is the case for the free deoxyribose (Serianni et al., 1990).

Connectivities from C7 to the α and β forms of D6 were observed by interresidue C7 aromatic to D6 ribose NOEs. The most downfield set of H_5 and H_6 protons of C7 can be directly correlated to the β form of the abasic site, and the most upfield H_5 and H_6 set of protons of C7 correspond to the α form. For the β form of the abasic site, NOEs were observed for the aromatic H_5 of C7 to the $H_{2'}$, $H_{2''}$, and $H_{3'}$ protons of D6 as well as from the aromatic H_6 of C7 to the $H_{2'}$ and $H_{1'}$ protons. A potential NOE from H_6 of C7 to the $H_{2''}$ of D6 is not resolvable. These NOEs are commonly observed in standard nondamaged B-DNA at these experimental mixing times. The connectivities from C7 to the α form are different than those observed for the β form. A NOE from the H_6 of C7 to the $H_{1'}$ proton of the α form is not observed, and this result is consistent with the position of the $H_{1'}$ proton of the α form. The observed connectivities from C7 to D6 include a NOE of very weak intensity from the aromatic H_5 of C7 to the $H_{2''}$ proton of D6 and a NOE to the $H_{3'}$ proton of the α form of D6. NOE cross-peaks for the aromatic H_6 of C7 to the $H_{2'}$ and $H_{2''}$ protons of the α form of D6 are not in a resolvable region, which makes it impossible at present to speculate on potential conformational and dynamical differences between the anomeric forms.

The α and β anomeric forms were also distinguished on the basis of the observation of $H_{1'}$ to $H_{3'}$ NOEs at the experimental mixing times. Only one of the anomeric forms exhibits a $H_{1'}$ to $H_{3'}$ NOE. At these mixing times, $H_{1'}$ to $H_{3'}$ NOEs are significantly influenced by spin diffusion and were observed for a majority of the residues. The β anomeric form has the $H_{1'}$ proton in the normal position relative to the other ribose protons, and it is thought that the $H_{1'}$ to $H_{3'}$ NOE observed is then due to the β form. This $H_{1'}$ proton also has a NOE to the H_6 proton of C7, and these results are therefore consistent with the β form of D6 described above.

The assignment of A17 was based on the NOE cross-peaks to the adjacent residues C18 and G16. These cross-peaks are analogous to those observed for B-form DNA and include the H_6 of C18 to the $H_{2''}$ and $H_{1'}$ protons of A17. Furthermore, there is connectivity from the H_8 of A17 to multiple forms of the $H_{1'}$ proton of G16. The presence of these cross-peaks indicates that the aromatic portion of A17 is stacked in the helix in a B-like manner. In support of the notion that A17 is stacked in the helix is the observation that there are no

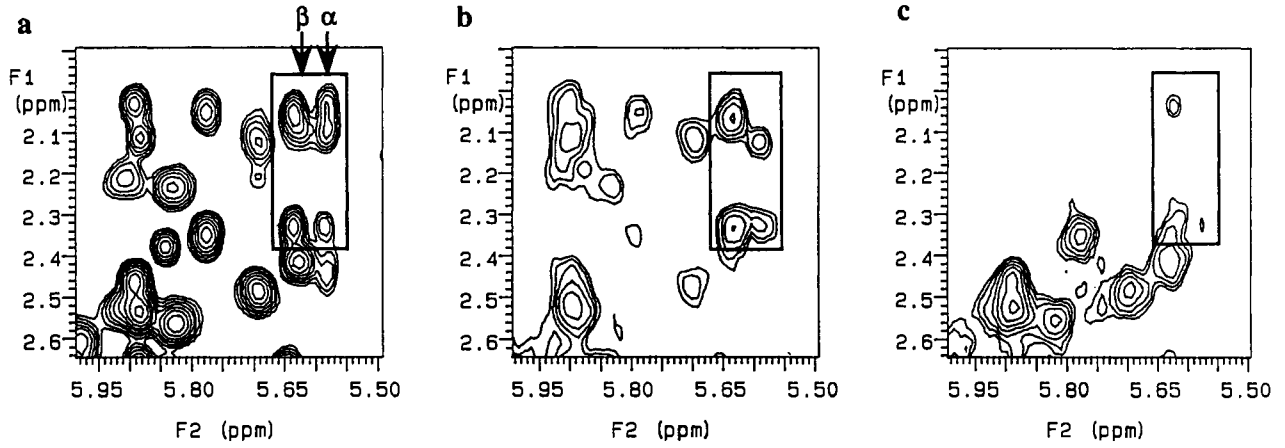

FIGURE 2: Two-dimensional NMR data for AD1 at 20 °C of the $H_{2'}/H_{2''}$–$H_{1'}$ region with the α and β anomeric forms indicated. In (a) is the 600-MHz NOESY spectrum obtained with a mixing time of 360 ms, in (b), the 400-MHz TOCSY spectrum obtained with a mixing time of 60 ms, and in (c), the 400-MHz ROESY spectrum obtained with a mixing time of 90 ms.

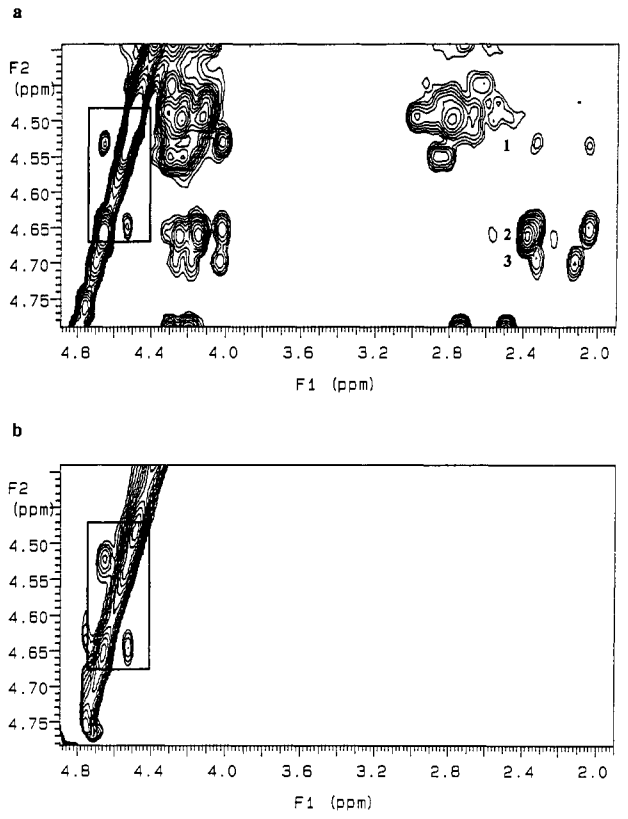

FIGURE 3: Cross-peaks indicated in the box represent the chemical exchange peaks for the two forms of the $H_{3'}$ proton of the β anomeric form of the abasic site. In (a) the positive contours of a 600-MHz NOESY spectra with a mixing time of 360 ms are shown. The three sets of the $H_{3'}$–$H_{2'}/H_{2''}$ cross-peaks for the abasic site are numbered with 1 and 2 corresponding to the minor and major forms of the $H_{3'}$ proton in the β anomeric form, which are in chemical exchange, and 3 representing the $H_{3'}$ signal from the α form. In (b) the positive contours of a 400-MHz ROESY spectra obtained with a mixing time of 90 ms are shown.

observable NOEs between C18 and G16, which can only occur if the A17 is extrahelical.

In the one-dimensional proton spectra of AD1, two sets of signals were observed for at least some of the protons of residues G5 and C18, D6 and A17, C7 and G16, and A4 and T15. The aromatic region of AD1, included in the supplementary material, exhibits multiple forms for some of the resonances. The one-dimensional spectrum for AU1 is also included in the supplementary material for comparison. For A4 and T15, the resolution of the two-dimensional data was not sufficient to resolve the two sets of signals. In all cases the chemical shift differences are small, less than 0.1 ppm. That is, multiple sets of signals were observed for the A-D pair as well as the adjacent *four* flanking base pairs. The two sets of signals correlate to the presence of the two anomeric configurations of the abasic site.

The differences in the intensities of the NOE cross-peaks associated with the two forms are apparently small, less than 20%, and indicate that the conformations of the two forms are similar. It also appears that the multiplicities observed for the A4 and T15 residues most likely arise from alterations in the ring current shifts experienced by protons at these sites from the adjacent G5, C18 and C7, G16 pairs as well as from A17. It is generally expected that chemical shift changes will be observed to at least one base pair further than the extent of the actual conformational differences due to changes in long-range ring current shifts.

The proton resonances of the corresponding DNA sample AU1 have also been assigned and are given in Table II. The comparison of the chemical shifts and NOEs of AD1 and AU1 indicates that the conformational differences between the two samples are localized to the lesion site and the two adjacent base pairs, with chemical shift differences extending to the AT pairs. On the basis of the proton assignments and proton–proton NOEs, the conformational effects of the abasic site are localized and do not extend throughout the duplex.

Imino Proton Exchange Rates of AD1, GD1, and AU1. The line widths of the imino protons of AD1, GD1, and AU1 were studied as a function of temperature to monitor the effect of the abasic site lesion on the helix opening rate (Gueron et al., 1987; Leroy et al., 1988; Pardi et al., 1982; Pardi & Tinoco, 1982) and a striking difference due to the presence of the abasic site was obtained. The imino proton spectra of AD1 and AU1 over the temperature range of 10–25 °C are shown in Figure 4. The spectra show that the imino protons of the AT pairs of AD1 have a much *lower* sensitivity to temperature than do those of the AU1 duplex and indicate a decreased rate of imino proton exchange at the base pairs two removed from the site of the lesion. This result is surprising in that the abasic site duplexes have a lower thermal melting point, T_m, as detected by optical methods, than the normal reference duplex by about 5 °C (Goljer and Bolton, manuscript in preparation). The imino proton melting of GD1 was found to be essentially the same as that for AD1 and is also shown in Figure 4.

Before these results were obtained, it was expected that the base pairs adjacent to the abasic site would have lifetimes significantly less than those of the control AU1 sample. The

Table II: AU1 Chemical Shift Assignments[a]

residue	H_8/H_6	H_5	$H_{1'}$	$H_{2'}$	$H_{2''}$	$H_{3'}$	$H_{4'}$	CH_3
C1	7.76	6.02	5.88	2.13	2.55	4.81	4.18	
G2	8.08		6.02	2.80	2.86	5.11	4.47	
C3	7.49	5.56	5.65	2.13	2.48	nya[b]	4.29	
A4	8.32		6.20	2.86	3.05	5.17	4.53	
G5	7.78		5.86	2.64	2.69	5.08	4.51	
U6	7.52	5.09	6.13	2.16	2.61	nya	4.36	
C7	7.60	5.76	5.56	2.13	2.47	nya	4.18	
A8	8.32		6.10	2.85	2.99	5.16	4.50	
G9	7.81		5.86	2.66	2.73	5.08	4.49	
C10	7.61	5.44	6.09	2.23	2.59	4.84	4.28	
C11	7.73	5.79	6.32	2.66	2.37	4.64	4.11	
G12	8.01		5.85	2.73	2.86	5.10	4.33	
G13	7.97		6.09	2.79	2.85	5.12	4.54	
C14	7.56	5.42	6.13	2.17	2.62	nya	4.36	
T15	7.40		5.76	2.12	2.46	4.47	4.22	1.72
G16	8.02		5.66	2.84	2.90	5.14	4.47	
A17	8.28		6.32	2.82	3.01	5.14	4.58	
C18	7.35	5.31	5.83	1.99	2.54	4.80	4.28	
T19	7.39		5.84	2.20	2.55	nya	nya	1.67
G20	8.01		5.96	2.75	2.79	5.10	4.47	
C21	7.46	5.55	5.90	2.02	2.46	nya	4.28	
G22	8.05		6.27	2.73	2.49	4.78	4.29	

[a] H_2O is referenced at 4.90 ppm. [b] nya, proton signal not yet assigned.

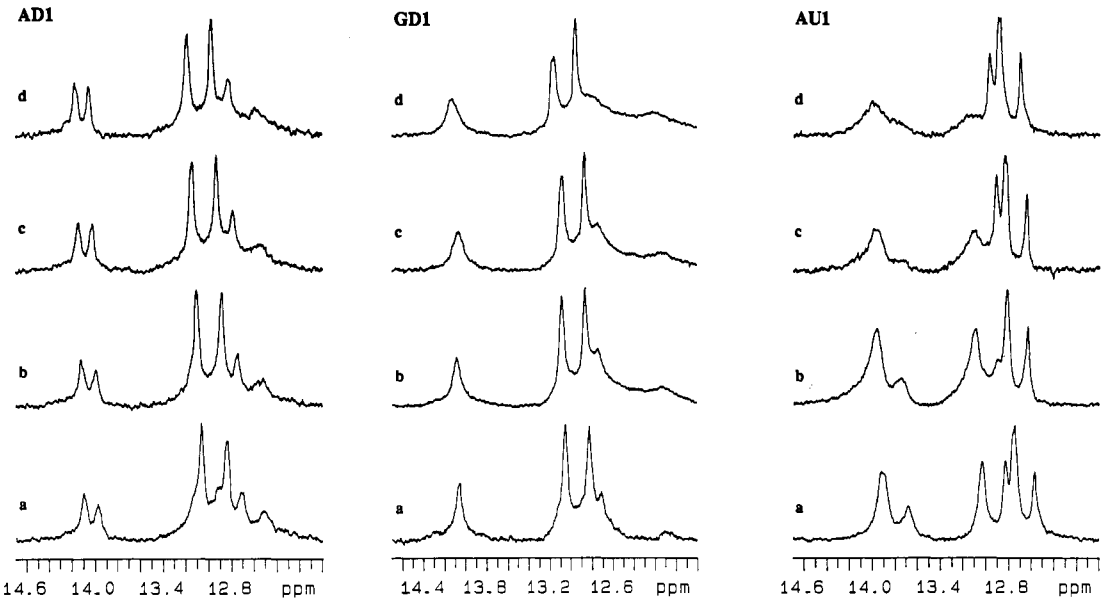

FIGURE 4: Spectra of the exchangeable imino protons of AD1, GD1, and AU1 obtained at 400 MHz at (a) 10 °C, (b) 15 °C, (c) 20 °C, and (d) 25 °C are shown. The imino protons can be observed between 13.5 and 14.5 ppm for the AT base pairs and between 11.5 and 13.3 ppm for the GC base pairs. These spectra show that in the presence of the abasic site the AT base pairs melt out at a higher temperature than is the case for the undamaged AU1 duplex.

lesion might be expected to enhance the rate of helix opening and hence increase the rate of imino proton exchange with solvent and thereby reduce the imino lifetime. This may be the first example of a decrease in thermal stability being associated with an increase in several imino lifetimes in residues in the interior of the duplex. No such behavior has been reported for DNA duplexes containing analogues of the abasic site. Thus, while the abasic site lesion does not appear to have a pronounced conformational effect, a striking effect on the helix opening dynamics of the DNA duplexes AD1 and GD1 does occur to at least two base pairs removed from the lesion site.

^{31}P and ^{31}P–^{1}H Correlation Data of AD1, GD1, and AU1. The ^{31}P spectra of AD1, GD1, and AU1 are shown in Figure 5. The spectra of AD1 and GD1 have all of the resonances in the region associated with B-form DNA with two resonances downfield to the main cluster of signals. Quantitative integration of the downfield signals was not possible due to the spectral overlap, but the total intensity of the two downfield signals is about one resonance with the general intensity distribution of the AD1 and GD1 spectra being quite similar.

The assignment of one of these downfield signals in AD1 was obtained via a ^{31}P–^{1}H correlation experiment. These results show the phosphorus signal at −2.37 ppm is correlated with the $H_{3'}$ at 4.65 ppm of the β anomeric form of the abasic site (see supplementary material). The phosphorus signal for the α configuration of the abasic site was not resolved in the heteronuclear correlation experiment. The ^{31}P chemical shifts and heteronuclear correlation are thus in agreement, with the proton results indicating some localized distortion near the lesion site. As discussed below, these ^{31}P results are rather different from those obtained on DNA duplexes containing analogues of the abasic site.

In AD1, there is an additional small phosphorus signal at −2.06 ppm that is not correlated to a $H_{3'}$ proton. The T_1 for this resonance as well as the ^{31}P–^{1}H coupling constants de-

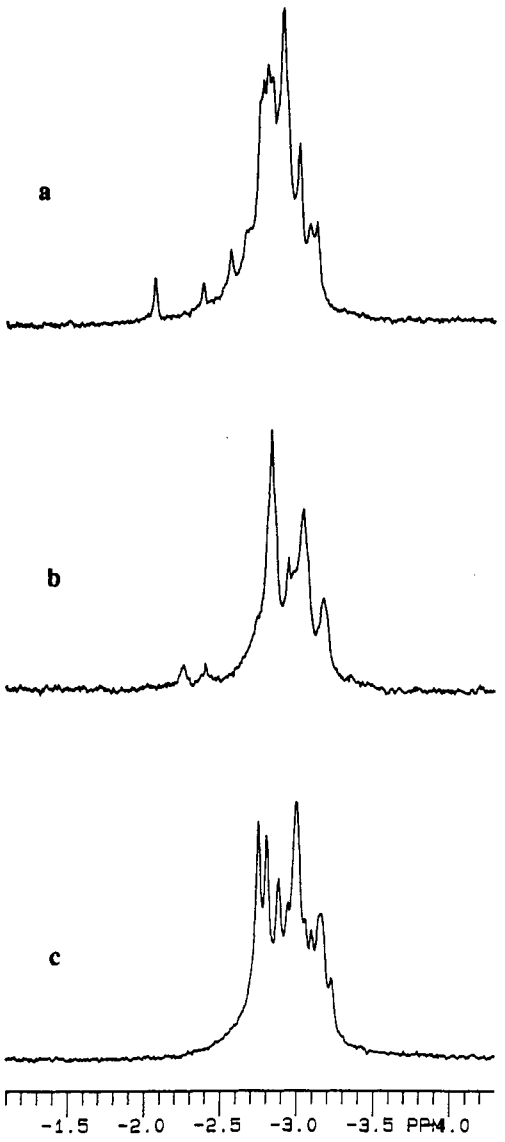

FIGURE 5: Proton-decoupled ^{31}P spectra of (a) AD1, (b) GD1, and (c) AU1 obtained at 161 MHz with the samples at 20 °C are shown. The spectra are referenced to the phosphate buffer at 0.0 ppm.

termined via the heteronuclear experiment are sufficiently different from any other DNA signals so that the phosphorus signal at−2.06 ppm is not assigned to the DNA duplex.

Comparison of NMR Results on AD1 and GD1. The proton NMR spectra of GD1 were analyzed in the manner described above for AD1, with the assignments given in the supplementary material. The basic features are the same as those found for AD1, with the conformational effect of the lesion being restricted to the lesion site and the two adjacent base pairs and the chemical shift changes extending one base pair further. There are two sets of signals for the residues at the lesion site and at least one of the bases in the four adjacent base pairs. In GD1, multiple signals are not resolvable for G16 and G5 in the two-dimensional spectra, unlike those observed in AD1.

The environment of D6 appears to be analogous in AD1 and GD1 on the basis of the chemical shifts of the $H_{1'}$, $H_{2'}$, $H_{2''}$, and $H_{3'}$ protons, with the exception that multiple signals for the $H_{3'}$ proton of the β form are not observed. Furthermore, G17 in GD1 appears to have different properties than does A17 in AD1. Whereas A17 had the normal B-form DNA NOEs to G16 and C18, no such signals are observed from G17 since no detectable signal from G17 could be found, suggesting

Chart I

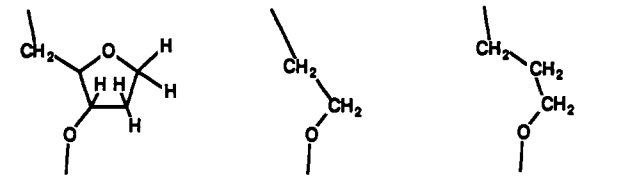

that G17 may be disordered due to slow to moderate exchange rates between two or more states. No NOEs are observed between C18 and G16, which would indicate an extrahelical G17. However, G17 could spend some of the time in an extrahelical position such that there would be no observable C18 ⇔ G16 NOEs.

The following results suggest that G17 is stacked and is interconverting between forms that have similar conformations but different chemical shifts. If G17 were equilibrating between significantly different conformations, then the ring current shifts of the nearby residues would reflect this. However, the resonances of C18 and C7 have line widths comparable to those in AD1 and AU1 and show splittings (due to the two hemiacetal forms) analogous to those observed in AD1. Furthermore, the imino proton spectra of GD1 shown in Figure 4 indicate the same longer imino proton lifetimes as found for AD1, which suggests a reduced helix opening rate, whereas an interconversion between a stacked and extrahelical G17 would be more compatible with a more rapid helical opening.

The NOE results, the chemical shift differences between the resonances associated with the two hemiacetal forms, the extent of conformational disruption due to presence of the lesion, and the reduced rate of imino proton exchange of the GD1 duplex are very similar to those of AD1. The major difference is that whereas A17 has NOEs to G16 and C18, consistent with B-form DNA, G17 appears to exhibit local disorder.

Comparison of Results on Aldehydic Lesions and Analogues Thereof. There have been prior investigations of DNA duplexes containing analogues of the abasic site. These studies have investigated the tetrahydrofuran analogue (V), referred to here as Th, the acyclic ethanyl analogue (VI), and the acyclic propanyl analogue (VII), which are illustrated in Chart I. There have been two independent groups that have reported on the Th analogue. The results from Patel and co-workers (Kalnik et al., 1988, 1989) have indicated that the presence of V, VI, or VII induces considerable distortion in the DNA duplexes of nine base pairs in length, as evidenced by ^{31}P and proton NMR studies. The ^{31}P NMR spectrum of the Th-containing DNA duplex has three resonances that are downfield from the main cluster and include the phosphates 5′ and 3′ to the abasic site as well as the phosphate 3′ to the base opposite the abasic site. Downfield signals are also observed with the propanyl- and ethanyl-containing DNA duplexes from the corresponding three sites. This is in contrast to the more normal resonance positions observed for the aldehydic abasic site. In addition, the dA-Th pair apparently is in a non-B-like conformation. Thermodynamic investigations (Vesnaver et al., 1989) on the same modified sequences described above with two additional dC-dG base pairs on both ends indicate a significant decrease in duplex stability relative to the unmodified sequence, as determined by a reduction in the transition temperature of approximately 14 °C.

An independent investigation of a different 9-mer DNA duplex containing a dA-Th pair indicated that the DNA is

basically B-DNA without significant distortion in the region of the lesion and that the imino protons exhibited behavior expected for B-DNA (Cuniasse et al., 1987). A subsequent examination of the same sequence with a dG-Th pair indicated that the dA-Th and dG-Th pairs are structurally similar at low temperature but do have some differences in their melting behavior (Cuniasse et al., 1990). The dC-Th and dT-Th pairs appear to have distinctly different structures than the purine-Th pairs.

The differences in the two sets of results on the dA-Th-containing DNAs may be due to the different sequence contexts that were investigated. However, neither sequence context appears to have properties that are similar to those we have observed for DNA containing aldehydic abasic sites.

Comparison of Aldehydic Lesions with Undamaged DNA. The results presented above indicate that the conformation of duplex DNA is somewhat altered by the presence of an aldehydic abasic site, with the extent of the disruption extending to the immediately adjacent base pairs. This disruption can be observed as multiple sets of signals that correspond to α and β anomeric forms of the abasic site. The extent of the conformational disruption has not been completely quantified, but the disruption appears to be relatively small in the case of AD1 as indicated by proton–proton NOE, TOCSY, and ROESY data as well as the ^{31}P chemical shifts and ^{31}P–^{1}H correlations.

The largest effect of the introduction of the abasic site lesion appears to be in the dynamics of the DNA duplex, with the imino exchange rates becoming much slower for internal AT base pairs in the damaged DNA than in the undamaged DNA. At an abasic site the volume usually occupied by the base is occupied by water molecules. If these water molecules are highly ordered, as appears likely, then the entropy of activation cost associated with transient opening of the helix could be larger than the entropy cost of opening an undamaged helix. Preliminary molecular dynamics modeling of the abasic site indicates that two or three water molecules occupy this space, and the activation entropy associated with "melting" this number of ordered water molecules could be large enough to account for the reduced rate of helical opening.

The slow helix opening may contribute to the protection of abasic sites from base-catalyzed hydrolysis. We have previously shown that the percentage of the aldehyde form is the same, about 1%, for the free deoxyribose and for the abasic site in duplex DNA (Wilde et al., 1989). It was concluded that the protection of the abasic sites from hydrolysis is by exclusion of the base catalyst from the abasic site. Thus, the relatively slow helix opening may offer protection from hydrolysis by exclusion of base from the abasic site.

The results on GD1 are very similar to those obtained on AD1 and do not indicate any pronounced differences except that G17 appears to be disordered whereas A17 is not. GD1 has the same extent of disruption, slower rate of imino proton exchange, and other properties of AD1. The preference for which base is placed opposite the abasic site is determined by the transition state of the DNA–DNA polymerase complex in the rate-determining step. At this time it is not apparent that there is sufficient difference between the interactions of dA and dG with abasic sites, in the context of double-stranded DNA, to explain the preference for dA to be placed opposite the abasic site by DNA polymerase.

Summary. The above results indicate several important features of DNA duplexes containing abasic sites. The extent and magnitude of conformational change is apparently small for AD and GD pairs, and the presence of abasic sites has a pronounced effect on the helix opening rate. The properties of duplexes containing aldehydic abasic sites are rather different from those having analogues of the abasic site, and it appears that the analogues of the abasic site studied to date are not reliable models of the aldehydic abasic site. Future studies are planned to incorporate the NMR data with molecular modeling along the lines we have recently described (Withka et al., 1991; Swaminathan et al., 1991) to obtain a detailed picture of the structure and mobility at the abasic site, to investigate pyrimidine-abasic site pairs, and to more completely characterize the differences in dynamics between abasic site containing DNA and undamaged DNA, which may be important in determining the stability of the damaged DNAs to base-catalyzed hydrolysis.

Acknowledgments

The 600-MHz spectra were obtained with the kind assistance of Drs. George Gray and Paul Kiefer of Varian Associates.

Supplementary Material Available

Four figures, showing the H_5 to H_6 region of the 400-MHz DQF-COSY spectrum of AD1, the heteronuclear ^{31}P–^{1}H spectrum of AD1, the $H_{2'}/H_{2''}$–$H_{1'}$ region of the 600-MHz NOESY spectrum of AD1, and the aromatic region of the 400-MHz ^{1}H NMR spectra of AD1 and AU1, and one table, showing GD1 chemical shift assignments (5 pages). Ordering information is given on any current masthead page.

References

Bax, A., & Davis, D. G. (1985) *J. Magn. Reson. 63*, 207–213.
Bolton, P. H. (1991) *Prog. Nucl. Magn. Reson. Spectrosc. 22*, 423–452.
Bothner-By, A. A., Stevens, R. L., Lee, J., Warren, C. D., & Jeanloz, R. W. (1984) *J. Am. Chem. Soc. 106*, 811–813.
Braunschweiler, L., & Ernst, R. R. (1983) *J. Magn. Reson. 53*, 521–528.
Chazin, W. J., Wuthrich, K., Hyberts, S., Rance, M., Denny, W. A., & Leupin, W. (1986) *J. Mol. Biol. 190*, 439–453.
Clore, G. M., & Gronenborn, A. M. (1989) *CRC Crit. Rev. Biochem. Mol. Biol. 24*, 479–564.
Cuniasse, Ph., Sowers, L. C., Eritja, R., Kaplan, B., Goodman, M. F., Cognet, J. A. H., LeBret, M., Guschlbauer, W., & Fazakerley, G. V. (1987) *Nucleic Acids Res. 15*, 8003–8022.
Cuniasse, Ph., Fazakerley, G. V., Guschlbauer, W., Kaplan, B. E., & Sowers, L. C. (1990) *J. Mol. Biol. 213*, 303–314.
Ernst, R. R., Bodenhausen, G., & Wokaun, A. (1987) *Principles of Nuclear Magnetic Resonance in One and Two Dimensions*, Clarendon Press, Oxford, England.
Friedberg, E. C. (1985) *DNA Repair*, W. H. Freeman, New York.
Goldberg, I. H. (1987) *Free Radical Biol. Med. 3*, 41–54.
Gueron, M., Kochoyan, M., & Leroy, J. L. (1987) *Nature 328*, 89–92.
Hore, P. J. (1983) *J. Magn. Reson. 55*, 283–300.
Kalnik, M. W., Chang, C. N., Grollman, A. P., & Patel, D. J., (1988) *Biochemistry 27*, 924–931.
Kalnik, M. W., Chang, C. N., Johnson, F., Grollman, A. P., & Patel, D. J. (1989) *Biochemistry 28*, 3373–3383.
Kappen, L. S., Goldberg, I. H., Frank, B. L., Worth, L., Christner, D. F., Kozarich, J. W., & Stubbe, J. (1991) *Biochemistry 30*, 2034–2042.
Kozarich, J. W., Worth, L., Frank, B. L., Christner, D. F., Vanderwall, D. E., & Stubbe, J. (1989) *Science 245*, 1396–1399.

Leroy, J. L., Kochoyan, M., Huynh-Dinh, T., & Gueron, M. (1988) *J. Mol. Biol. 60*, 223-238.
Lindahl, T. (1982) *Annu. Rev. Biochem. 51*, 61-87.
Loeb, L. A., & Preston, D. B. (1987) *Annu. Rev. Genet. 20*, 201-230.
Manoharan, M., Ransom, S. C., Mazumder, A., Gerlt, J. A., Wilde, J. A., Withka, J. M., & Bolton, P. H. (1988a) *J. Am. Chem. Soc. 110*, 1620-1622.
Manoharan, M., Mazumder, A., Ransom, S. C., Gerlt, J. A., & Bolton, P. H. (1988b) *J. Am. Chem. Soc. 110*, 2690-2691.
Mazumder, A., Gerlt, J. A., Rabow, L., Absalon, M. J., Stubbe, J., & Bolton, P. H. (1989) *J. Am. Chem. Soc. 111*, 8029-8030.
Mazumder, A., Gerlt, J. A., Absalon, M. J., Stubbe, J., Cunningham, R. P., Withka, J. M., & Bolton, P. H. (1991) *Biochemistry 30*, 1119-1126.
Pardi, A., & Tinoco, I. (1982) *Biochemistry 21*, 4686-4693.
Pardi, A., Morden, K. M., Patel, D. J., & Tinoco, I. (1982) *Biochemistry 21*, 6567-6574.
Randall, S. K., Eritja, R., Kaplan, B. E., Petruska, J., & Goodman, M. F. (1987) *J. Biol. Chem. 262*, 6864-6870.
Sagher, D., & Strauss, B. (1983) *Biochemistry 22*, 4518-4526.
Schaaper, R. M., Kunkel, T. A., & Loeb, L. A. (1983) *Proc. Natl. Acad. Sci. U.S.A. 80*, 487-491.
Serianni, A. S., Kline, P. C., & Snyder, J. R. (1990) *J. Am. Chem. Soc. 112*, 5886-5887.
Shaka, A. J., Keeler, J., & Freeman, R. (1983) *J. Magn. Reson. 53*, 313-340.
Shaka, A. J., Lee, C. J., & Pines, A. (1988) *J. Magn. Reson. 77*, 274-293.
States, D. J., Haberkorn, R. A., & Ruben, D. J. (1982) *J. Magn. Reson. 48*, 286-292.
Swaminathan, S., Ravishanker, G., & Beveridge, D. L. (1991) *J. Am. Chem. Soc. 113*, 5027-5040.
Vesnaver, G., Chang, C., Eisenberg, M., Grollman, A. P., & Breslauer, K. J. (1989) *Proc. Natl. Acad. Sci. U.S.A. 86*, 3614-3618.
Wemmer, D. E., & Reid, B. R. (1985) *Annu. Rev. Phys. Chem. 35*, 105-137.
Wilde, J. A., Bolton, P. H., Mazumber, A., Manoharan, M., & Gerlt, J. A. (1989) *J. Am. Chem. Soc. 111*, 1894-1896.
Withka, J. M., Swaminathan, S., Beveridge, D. L., & Bolton, P. H. (1991) *J. Am. Chem. Soc. 113*, 5041-5049.
Wüthrich, K. (1986) *NMR of Proteins and Nucleic Acids*, John Wiley & Sons, New York.

Mg^{2+}, Asp^-, and Glu^- Effects in the Processive and Distributive DNA Relaxation Catalyzed by a Eukaryotic Topoisomerase I†

P. Arsène Der Garabedian,* Gilles Mirambeau,‡ and Jacqueline J. Vermeersch
Laboratoire d'Enzymologie, Université Pierre et Marie Curie, URA 554 CNRS, 96 Boulevard Raspail, 75006 Paris, France
Received May 3, 1991; Revised Manuscript Received July 18, 1991

ABSTRACT: The salt requirement for the catalysis of DNA relaxation carried out by a eukaryotic DNA topoisomerase I from *Candida* was reexamined with plasmid pBR322 DNA. Two levels of analysis were considered: the initial velocity of the overall reaction and the mode of this reaction (processivity vs distributivity). When looking at the monovalent salts from the first level, the replacement of Cl^- by Glu^- or Asp^- greatly enhanced the salt range over which the enzyme was active. Moreover, the initial velocity reached an optimal value for a higher salt concentration in this case. For the cationic counterpart, K^+ was a little more effective than Na^+ and much more so than NH_4^+. Addition of 4 mM magnesium chloride affected both the range and the optimum of the initial velocity differentially, depending upon the monovalent salt, but with a general stimulating tendency. On the other hand, when the Mg^{2+} salt was varied, substitution of chloride by aspartate enhanced the optimum of the initial velocity for a fixed KCl concentration. In addition, magnesium aspartate ($MgAsp_2$) and magnesium glutamate ($MgGlu_2$) allowed the reaction to occur even without monovalent salt and over an extended range. Magnesium was also shown to directly interact with the general catalysis (K_d = 2.5 mM). From the second level of analysis, the presence of Mg^{2+} (except with NH_4Glu), the substitution of Cl^- by Glu^- or Asp^-, and a lower monovalent salt concentration than that used for the velocity optimum were required to promote the processive mode. The mode of action of magnesium as well as the interest of the substitution of the chloride ion by glutamate or aspartate are discussed. Finally, the data derived from both analyses are supported by the proposed existence of an intermediary complex between supercoiled DNA, Mg^{2+}, and DNA topoisomerase I, which may explain the processive relaxation of supercoils into DNA (presumably the predominant in vivo catalysis).

DNA topoisomerases (topo) are enzymes that alter the topological states of DNA. They can be divided in two classes (topo I and topo II), depending upon their mode of action, and are widely distributed in prokaryotes and eukaryotes. It is now well established that these enzymes play a crucial role in most of the biological processes involving DNA (Wang, 1985; Osheroff, 1989).

The eukaryotic type I topoisomerase has been studied extensively since its discovery in 1972 (Champoux & Dulbecco, 1972). Its prominent catalytic activity, i.e., DNA relaxation, can be summarized as follows: after binding to some preferential site on the DNA, topo I efficiently acts by creating a transient break in one strand and by promoting the passage

† This work was supported by grants from CNRS.
* To whom correspondence should be addressed.
‡ Present address: Unité de Physicochimie des Macromolécules Biologiques, Institut Pasteur, 75724 Paris Cedex 15, France.

0006-2960/91/0430-9940$02.50/0